

## Scaling of Spontaneous Rotation with Temperature and Plasma Current in Tokamaks

F. I. Parra,<sup>1,2,\*</sup> M. F. F. Nave,<sup>3,1</sup> A. A. Schekochihin,<sup>1</sup> C. Giroud,<sup>4</sup> J. S. de Grassie,<sup>5</sup> J. H. F. Severo,<sup>6</sup>  
P. de Vries,<sup>7</sup> and K.-D. Zastrow<sup>4</sup>

<sup>1</sup>Rudolf Peierls Centre for Theoretical Physics, University of Oxford, Oxford OX1 3NP, UK

<sup>2</sup>Plasma Science and Fusion Center, Massachusetts Institute of Technology, Cambridge, Massachusetts 02139, USA

<sup>3</sup>Associação EURATOM/IST, Instituto de Plasmas e Fusão Nuclear, Instituto Superior Técnico,  
Technical University of Lisbon, Portugal

<sup>4</sup>Euratom/CCFE Fusion Association, Culham Science Centre, Abingdon OX14 3DB, United Kingdom

<sup>5</sup>General Atomics, P.O. Box 85608, San Diego, California, USA

<sup>6</sup>Institute of Physics, University of São Paulo, SP, Brazil

<sup>7</sup>FOM Institute for Plasma Physics, Rijnhuizen, Association EURATOM-FOM, Nieuwegein, The Netherlands

(Received 30 August 2011; published 29 February 2012)

Using theoretical arguments, a simple scaling law for the size of the intrinsic rotation observed in tokamaks in the absence of a momentum injection is found: The velocity generated in the core of a tokamak must be proportional to the ion temperature difference in the core divided by the plasma current, independent of the size of the device. The constant of proportionality is of the order of  $10 \text{ km} \cdot \text{s}^{-1} \cdot \text{MA} \cdot \text{keV}^{-1}$ . When the intrinsic rotation profile is hollow, i.e., it is countercurrent in the core of the tokamak and cocurrent in the edge, the scaling law presented in this Letter fits the data remarkably well for several tokamaks of vastly different size and heated by different mechanisms.

DOI: 10.1103/PhysRevLett.108.095001

PACS numbers: 52.25.Fi, 52.30.-q, 52.55.Fa

*Introduction.*—Because of their axisymmetry, tokamak plasmas can be made to rotate at high speeds if momentum is injected into them. If the rotation is sufficiently large, large scale magnetohydrodynamic instabilities are stabilized [1] and the turbulent transport of energy can be much reduced [2–4]. Unfortunately, ITER [5], the largest magnetic confinement experiment currently being built, is not expected to have an effective momentum deposition due to its size and high density. As a result, there has been mounting interest in the intrinsic, or spontaneous, rotation observed in tokamaks without momentum injection [6]. If this intrinsic rotation could be made large, it could be used to prevent instabilities and reduce turbulence as is done with momentum injection. Understanding the origin of this rotation is also an interesting physics question. This has driven several experimental [6–10], numerical [11–13], and theoretical [14–17] studies. So far, numerical results for intrinsic rotation have only been obtained using global gyrokinetic simulations that have been recently proven to be flawed for radial momentum transport in the core of tokamaks [18].

In this Letter, we use very simple theoretical arguments to show that the velocity difference within the core of a tokamak must scale proportionally to the ion temperature divided by the plasma current. The constant of proportionality is independent of the machine size and is of order  $c^2/e = 10 \text{ km} \cdot \text{s}^{-1} \cdot \text{MA} \cdot \text{keV}^{-1}$ , where  $c$  is the speed of light and  $e$  is the proton charge. We show that pulses with hollow intrinsic rotation (countercurrent rotation at the magnetic axis and cocurrent at the edge) from machines whose sizes range from tens of centimeters to several

meters, that have very different plasma currents (from 0.1 to 2.5 MA), and that are heated by different mechanisms (JET [10], DIII-D [9], TCABR [19], and TCV [7]) follow the theoretical scaling.

*Theoretical arguments.*—In a tokamak plasma, turbulence and collisions transport momentum across magnetic surfaces. Momentum can be injected with neutral beams and radio frequency (rf) waves [20], but in many occasions there is no external source of momentum. When the latter is the case, the toroidal angular momentum flux  $\Pi$  through every flux surface must be zero, even though significant rotation can often be observed experimentally. Only the angular momentum in the toroidal direction is relevant. In the poloidal direction, the flow is strongly damped by collisional processes, which pass the momentum through the magnets to the structure of the tokamak. Thus, to calculate intrinsic rotation profiles, it is necessary to calculate the dependence of  $\Pi$  on the toroidal rotation frequency  $\Omega_\phi$  and then solve the equation  $\Pi(\Omega_\phi) = 0$  for  $\Omega_\phi$ .

Both turbulence and collisions occur on time scales that are longer than the inverse of the gyrofrequency, which means that the particle trajectories can be understood as a fast gyromotion around guiding centers, which move fast along magnetic field lines and drift slowly across them. This is the physical idea underlying gyrokinetics, which is the most commonly used approximation in transport simulations [21–25].

Even in the absence of turbulence and collisions, particles move out of the surface of constant magnetic flux where they started due to the  $\nabla B$  and curvature drifts,

but they remain within a given distance of it. This distance is of the order of the poloidal gyroradius  $\rho_\theta = mc v_{\text{th}}/eB_\theta$ , where  $e$  and  $m$  are the charge and mass of the particle,  $v_{\text{th}}$  is the thermal speed, and  $B_\theta$  is the poloidal component of the magnetic field. Note that  $\rho_\theta = (B/B_\theta)\rho$ , where  $\rho$  is the particle gyroradius and  $B$  is the total magnetic field. In most tokamaks,  $B/B_\theta$  is of order 10. Tokamaks are constructed so that  $\rho_\theta \ll L_T$ , where  $L_T$  is the characteristic length of the variation of the temperature  $T$ , which we use as our length of reference.

Collisions cause transport, known as neoclassical transport [26], because each collision makes the particle move from one drift orbit to another separated by  $\rho_\theta$ . Turbulent transport is caused by electromagnetic fluctuations, of which the most virulent are believed to be driven by the ion temperature gradient (ITG). For ITG turbulence well above marginality, the characteristic correlation length is  $(B/B_\theta)(a/L_T)\rho \sim \rho_\theta$ , where  $a$  is the minor radius of the tokamak ( $L_T \sim a$ ). This scaling is not based on the drift orbits as is in the case of collisional transport, but on the critical balance between the parallel and the perpendicular dynamics [27]. It is observed in experiments that the turbulent transport scales approximately linearly with  $B/B_\theta$  [28], as predicted by critical balance [27].

In general, tokamaks are geometrically up-down symmetric to a great degree in the core. In such tokamaks, to lowest order in  $\rho_\theta/L_T$ , the transport of momentum can only be different from zero if a preferred direction is given by either rotation or rotational shear. The lowest-order cancellation of the radial momentum flux in the absence of rotation is due to a fundamental symmetry of the turbulence and the particle motion [29–31]. Here we are assuming  $\Omega_\phi \sim v_{\text{th}}/R$ , this being the ordering for which the rotation and its shear enter in the lowest-order gyrokinetic equation [32,33]. Thus, schematically, to lowest order in  $\rho_\theta/L_T$ ,

$$\Pi \sim -\nu_t R^2 \left( \frac{\partial \Omega_\phi}{\partial r} + \frac{\Omega_\phi}{\ell_{\text{pinch}}} \right) - \nu_c R^2 \frac{\partial \Omega_\phi}{\partial r}, \quad (1)$$

where  $r$  is the radial coordinate,  $R$  is the major radius,  $\nu_t$  is the turbulent viscosity,  $-\nu_t/\ell_{\text{pinch}}$  is the turbulent pinch of momentum [34,35], and  $\nu_c$  is the collisional viscosity. Equation (1) has the main features of momentum transport in up-down symmetric tokamaks: Momentum transport can only happen when  $\Omega_\phi \neq 0$  or  $\partial \Omega_\phi/\partial r \neq 0$ , and it changes sign when  $\Omega_\phi$  and  $\partial \Omega_\phi/\partial r$  do [31]. It can be thought of as a Taylor expansion of the complicated function  $\Pi(\partial \Omega_\phi/\partial r, \Omega_\phi)$  around  $\Omega_\phi = 0$  and  $\partial \Omega_\phi/\partial r = 0$ .

The equation for intrinsic rotation is  $\Pi = 0$ , and with the lowest-order expression (1) for  $\Pi$ , the solution is  $\Omega_\phi \propto \exp[-\int dr \ell_{\text{pinch}}^{-1} (1 + \nu_c/\nu_t)^{-1}]$ . It is then possible to obtain intrinsic rotation if rotation is generated in some region of the plasma (for example, in the edge) and pinched to other regions. However, this mechanism is not fully

satisfactory because it cannot explain the variety of observed profiles [10]. In particular,  $\Omega_\phi$  cannot change sign, contradicting experimental observations (as we will show in the next section). Unfortunately, to lowest order, Eq. (1) is correct and no other mechanism for intrinsic rotation can be obtained.

If the expansion in  $\rho_\theta/L_T \ll 1$  is continued to next order, the rotation and its shear are not the only physical factors that provide a preferred direction and can give raise to momentum transport: The pressure and temperature gradients also break the up-down symmetry. Consider the guiding centers of two particles (1 and 2) that at point  $A$  at the outboard midplane of a tokamak have velocities in opposite directions, as sketched in Fig. 1. The dashed line represents the cut of a surface of constant magnetic flux through a poloidal plane (the axis of symmetry is the dash-dotted line). The poloidal magnetic field  $B_\theta$  is parallel to the dashed line and points counterclockwise, whereas the toroidal magnetic field  $B_\phi$  points toward the reader. At point  $A$ , particle 1 (red orbit) travels counterclockwise, and since to lowest order it follows the magnetic field, its toroidal velocity  $v_{\phi 1}$  is pointing towards the reader. Particle 2 (blue orbit) travels in the opposite direction both poloidally and toroidally. Orbits separate from the flux surface a small distance of order  $\rho_\theta$ . Particle 1 moves toward the center of the tokamak because its poloidal velocity is counterclockwise. Particle 2 drifts outwards. Because of the temperature gradient, the center of the tokamak is hotter, and particles like particle 1 will have more energy, of the order of  $(\rho_\theta/L_T)mv_{\text{th}}^2$ , breaking the symmetry and, in this simplified picture, making the plasma rotate counterclockwise poloidally, and toward the reader toroidally. Figure 1 shows that whereas the direction of the magnetic field is unimportant, the vector  $\mathbf{B} \times \nabla T$  does give a preferred direction at higher order in  $\rho_\theta/L_T$  parallel to or against which the plasma will tend to rotate. The mechanism described here does not determine the sense of the toroidal rotation, but it does demonstrate that background gradients break the up-down symmetry and that the effects of this symmetry breaking are of order  $\rho_\theta/L_T$ . Calculating all these effects is a rather

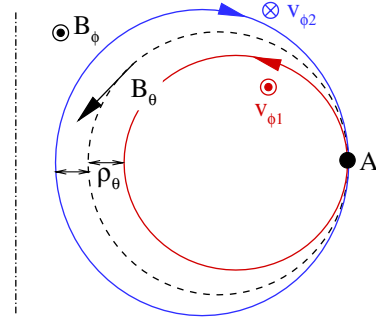


FIG. 1 (color online). Sketch of drift orbits.

sophisticated analytical task, involving many factors subtler than the simple argument given above [36].

The next-order contributions to momentum transport in  $\rho_\theta/L_T \ll 1$  were first calculated in neoclassical theory [37,38], where they are proportional to radial derivatives of the ion temperature. Models to calculate the next-order contributions to turbulent transport have also been proposed [16,17]. Near marginality, the turbulence amplitude is small, and the neoclassical corrections to the distribution function of order  $\rho_\theta/L_T$  due to finite drift orbit size are the dominant mechanism that breaks the up-down symmetry of the turbulence. Well above marginality, the characteristic eddie size is  $\rho_\theta$  [27], allowing the turbulence to sample regions in which the temperature gradient differs by  $\rho_\theta/L_T$ , and breaking the symmetry this way. In general, we expect the new next-order terms to depend strongly on density and temperature gradients because these drive the turbulence. Schematically, as shown in [17], we may write

$$\begin{aligned} \Pi \sim & -\nu_i R^2 \left[ \frac{\partial \Omega_\phi}{\partial r} + \frac{\Omega_\phi}{\ell_{\text{pinch}}} + O\left(\frac{\rho_\theta}{L_T} \frac{v_{th}}{RL_T}\right) \right] \\ & - \nu_c R^2 \left[ \frac{\partial \Omega_\phi}{\partial r} + O\left(\frac{\rho_\theta}{L_T} \frac{v_{th}}{RL_T}\right) \right]. \end{aligned} \quad (2)$$

From (2), setting  $\Pi = 0$  and assuming that the scale length of  $\Omega_\phi$  is of order  $L_T$ , we obtain  $R\Omega_\phi \sim (\rho_\theta/L_T)v_{th} \sim (c/eB_\theta)(T/L_T)$ , where  $T = mv_{th}^2/2$  is the temperature. The poloidal magnetic field is given by the toroidal plasma current  $I_p$ ,  $B_\theta \sim I_p/cL_B$ , where  $L_B$  is the characteristic length of variation of  $B_\theta$ . Therefore,  $R\Omega_\phi \sim (L_B/L_T) \times (c^2/e)(T/I_p)$ . In the core,  $L_B$  and  $L_T$  are both of the order of the minor radius  $a$ , so the toroidal velocity is

$$V_\phi = R\Omega_\phi \sim \frac{c^2}{e} \frac{T}{I_p}. \quad (3)$$

This equation gives the scaling of intrinsic rotation in the core with the temperature and plasma current. It is *independent of machine size*. The dimensional constant of proportionality is  $c^2/e = 10 \text{ km} \cdot \text{s}^{-1} \cdot \text{MA} \cdot \text{keV}^{-1}$ .

*Experimental measurements.*—We now compare experimental data from different machines that show similarities in their intrinsic rotation profiles. In Fig. 2 two pulses from JET represent two distinct types of intrinsic rotation profiles: the ones in which the toroidal velocity increases from the magnetic axis toward the edge of the tokamak (red profile), which we call *hollow profiles*, and the ones in which it decreases (blue profile), which we call *peaked profiles* (the toroidal velocity is deemed positive if it is cocurrent). The two pulses in Fig. 2 have very different input power and plasma current, and they are only meant to be examples of the two types of velocity profiles. The peaked profiles need not have higher temperature gradients than the hollow profiles. The velocity at the edge is mostly cocurrent, and this seems to be common to all tokamaks with low magnetic ripple in the absence of momentum

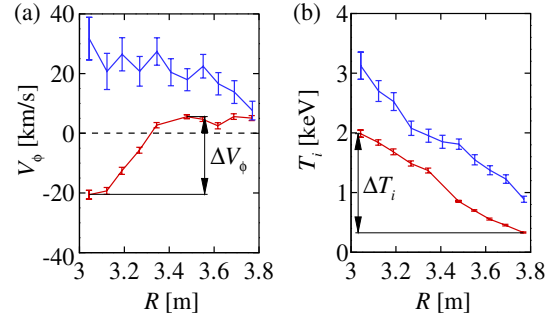


FIG. 2 (color online). Intrinsic rotation profiles (a) and ion temperature profiles (b) in JET plasmas with ICRH, pulses 66395 (red) and 74692 (blue). The rotation in the cocurrent direction is positive rotation. The position of the magnetic axis is around  $R = 3$  m; the separatrix is around  $R = 3.8$  m.

injection. In JET, the hollow profiles correspond to Ohmic shots and some of the ion cyclotron resonance heating (ICRH) pulses in both low-confinement mode ( $L$  mode) [10] and high-confinement mode ( $H$  mode) [39]. The cases with peaked profiles are all ICRH  $L$ -mode and  $H$ -mode shots.

To check (3), we compare the pulses with the hollow core velocity profile for four different tokamaks: JET [10], DIII-D [9], TCABR [19], and TCV [7]. To characterize the velocity generated intrinsically in the core, we use the difference in toroidal velocity  $\Delta V_\phi$  between the minimum of toroidal velocity closest to the magnetic axis on the outboard side and the first maximum encountered when moving from the magnetic axis toward the edge on the outboard side. This definition of  $\Delta V_\phi$  is illustrated in Fig. 2(a). The parameter  $\Delta V_\phi$  attempts to exclude any intrinsic velocity generated at the edge—most likely by means not covered in our theoretical discussion above. To give a measure of the sources generating intrinsic rotation in (2), we use the difference in ion temperature  $\Delta T_i$  between the magnetic axis and the temperature at the top of the pedestal in  $H$  modes, or the temperature measurement that is the closest to the separatrix in  $L$  modes. The difference  $\Delta T_i$ , illustrated in Fig. 2(b), excludes the ion temperature jump in the pedestal in the case of  $H$  modes. Figure 3 shows  $I_p \Delta V_\phi$  vs  $\Delta T_i$  for various tokamaks [40]. According to (3), we expect

$$I_p \Delta V_\phi = \alpha \frac{c^2}{e} \Delta T_i. \quad (4)$$

The dimensionless prefactor  $\alpha$  could not be determined in our qualitative theoretical discussion, but we can find its value from the present experimental analysis. The data are consistent with an approximate linear dependence with a slope of  $(18 \pm 4) \text{ km} \cdot \text{s}^{-1} \cdot \text{MA} \cdot \text{keV}^{-1}$  for all machines, giving  $\alpha \approx 1.8 \pm 0.4$ . The slope was determined by least-square fitting and the error is the 99% confidence interval. In Fig. 3 there are Ohmic, ICRH, and electron cyclotron

resonance heating (ECRH) shots,  $L$  and  $H$  modes, plasma currents spanning from 0.1 to 2.5 MA, and machines of sizes ranging from tens of centimeters (TCABR) to meters (JET). The fact that both the scaling and the prefactor seem to be valid for this variety of situations suggests that the theoretical ideas proposed above are robust.

When the same analysis was attempted for the peaked profiles in JET, the trend was not so clear, but we cannot conclude that the scaling is absent either. The study of peaked profiles will be the object of a future publication. Here we review several possible explanations for the lack of a clear scaling. In [8,12] a change from trapped electron mode (TEM) driven turbulence to ITG turbulence was proposed as the cause for the transition between peaked and hollow profiles. If this is the case,  $\Delta T_i$  is not a good parameter to work with because TEM turbulence depends strongly on the electron density gradient, for which  $\Delta T_i$  is not a good proxy, and on the electron temperature profile that for low collisionality may differ from  $T_i$ . It is also possible that the peaked-profile cases are dominated by the inward pinch of momentum generated at the edge [10], making the rotation in the core correlated to the parameters at the edge and not to the parameters of the core. With our preliminary analysis of peaked profiles in JET, we cannot decide if the transition from hollow to peaked profiles is due to the reasons given above, or other reasons not considered here. Experiments in DIII-D show that shaping affects intrinsic rotation, with high triangularity shots tending to have peaked profiles. Shaping may affect ITG and TEM turbulence differently, making one or the other type of turbulence dominant for high triangularity and hence deciding the direction of rotation in this way, or it may have an effect on the direction in which ITG or TEM turbulence pushes the plasma. Further study is needed. Even though the trend with  $\Delta T_i$  and  $I_p$  was not so clear, the velocity difference  $\Delta V_\phi$  was still of the same order as (3).

*Discussion.* Using simple theoretical arguments, we have shown that the intrinsic rotation generated in the core must scale according to (4). Hollow intrinsic rotation profiles from very different tokamaks follow this scaling. The scatter in Fig. 3 is to be expected since (4) is derived from an order of magnitude estimate and prefactors of order unity may vary from shot to shot.

There are ways of generating intrinsic rotation that have not been considered in this Letter. For example, in the core, rf heating can transport momentum [41,42] due to the large orbits of energetic ions. In the edge, direct particle losses can generate rotation [43]. It seems that these effects are not important in the cases presented in Fig. 3 because these include shots with and without energetic ions, and with and without a pedestal. We do not know how generic this is. We have introduced a dimensionless parameter  $\alpha = eI_p \Delta V_\phi / c^2 \Delta T_i$ , which was of order unity for a variety of regimes and machines considered here. It would be very instructive to quantify experimentally measured rotation in

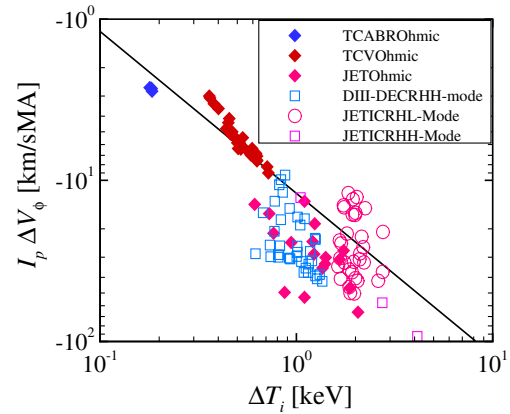


FIG. 3 (color online). Toroidal velocity difference in the core  $\Delta V_\phi$  multiplied by the plasma current  $I_p$  against the ion temperature difference  $\Delta T_i$  in the plasma core. The line is the least-square fit of the data to (4). The slope is  $18 \text{ km} \cdot \text{s}^{-1} \cdot \text{MA} \cdot \text{keV}^{-1}$ .

other cases in terms of this parameter. In cases that  $\alpha$  is significantly larger than unity, the rotation must have an external origin, such as energetic ions, edge effects, or momentum injection.

The experimental results presented above cannot determine if the transport of momentum is dominated by collisions or turbulence because both have the same scaling (3). Since turbulent viscosity is of the same order as the thermal diffusivity [35,44–47], and turbulent transport usually dominates, we expect the  $\rho_\theta/L_T$  corrections to the turbulent momentum transport to play the dominant role in driving intrinsic rotation.

The authors acknowledge many helpful discussions with M. Barnes and T. Johnson. This work was supported in part by EPSRC, STFC, Fundação para a Ciência e Tecnologia (FCT) of Portugal, the Leverhulme Trust Network for Magnetized Plasma Turbulence, the US DOE under DE-FC02-04ER54698, the European Communities through Association Euratom/IST, and carried out within the frameworks of the Instituto de Plasmas e Fusão Nuclear-Laboratório Associado and the European Fusion Development Agreement. The views and opinions expressed herein do not necessarily reflect those of the European Commission. This work was done under the JET-EFDA workprogramme [48].

\*fparra@mit.edu

- [1] P.C. de Vries *et al.*, *Plasma Phys. Controlled Fusion* **38**, 467 (1996).
- [2] J. W. Connor *et al.*, *Nucl. Fusion* **44**, R1 (2004).
- [3] P.C. de Vries *et al.*, *Nucl. Fusion* **49**, 075007 (2009).
- [4] P. Mantica *et al.*, *Phys. Rev. Lett.* **102**, 175002 (2009).
- [5] K. Ikeda *et al.*, *Nucl. Fusion* **47**, E01 (2007).
- [6] J.E. Rice *et al.*, *Nucl. Fusion* **47**, 1618 (2007).

- [7] A. Scarabosio *et al.*, *Plasma Phys. Controlled Fusion* **48**, 663 (2006).
- [8] B.P. Duval *et al.*, *Plasma Phys. Controlled Fusion* **49**, B195 (2007).
- [9] J. S. deGrassie *et al.*, *Phys. Plasmas* **14**, 056115 (2007).
- [10] L.-G. Eriksson *et al.*, *Plasma Phys. Controlled Fusion* **51**, 044008 (2009).
- [11] W. X. Wang *et al.*, *Phys. Plasmas* **17**, 072511 (2010).
- [12] Y. Camenen *et al.*, *Nucl. Fusion* **51**, 073039 (2011).
- [13] W. X. Wang, T. S. Hahm, S. Ethier, L. E. Zakharov, and P. H. Diamond, *Phys. Rev. Lett.* **106**, 085001 (2011).
- [14] P. H. Diamond *et al.*, *Phys. Plasmas* **15**, 012303 (2008).
- [15] Y. Camenen *et al.*, *Phys. Rev. Lett.* **102**, 125001 (2009).
- [16] F. I. Parra and P. J. Catto, *Plasma Phys. Controlled Fusion* **52**, 045004 (2010).
- [17] F. I. Parra, M. Barnes, and P. J. Catto, *Nucl. Fusion* **51**, 113001 (2011).
- [18] F. I. Parra and P. J. Catto, *Phys. Plasmas* **17**, 056106 (2010).
- [19] J. H. F. Severo *et al.*, *Nucl. Fusion* **43**, 1047 (2003).
- [20] A. Ince-Cushman *et al.*, *Phys. Rev. Lett.* **102**, 035002 (2009).
- [21] W. Dorland, F. Jenko, M. Kotschenreuther, and B. N. Rogers, *Phys. Rev. Lett.* **85**, 5579 (2000).
- [22] J. Candy and R. E. Waltz, *J. Comput. Phys.* **186**, 545 (2003).
- [23] T. Dannert and F. Jenko, *Phys. Plasmas* **12**, 072309 (2005).
- [24] A. G. Peeters *et al.*, *Comput. Phys. Commun.* **180**, 2650 (2009).
- [25] M. Barnes *et al.*, *Phys. Plasmas* **17**, 056109 (2010).
- [26] F. L. Hinton and R. D. Hazeltine, *Rev. Mod. Phys.* **48**, 239 (1976).
- [27] M. Barnes, F. I. Parra, and A. A. Schekochihin, *Phys. Rev. Lett.* **107**, 115003 (2011).
- [28] C. C. Petty, J. E. Kinsey, and T. C. Luce, *Phys. Plasmas* **11**, 1011 (2004).
- [29] A. G. Peeters and C. Angioni, *Phys. Plasmas* **12**, 072515 (2005).
- [30] H. Sugama *et al.*, *Plasma Phys. Controlled Fusion* **53**, 024004 (2011).
- [31] F. I. Parra, M. Barnes, and A. G. Peeters, *Phys. Plasmas* **18**, 062501 (2011).
- [32] M. Artun and W. M. Tang, *Phys. Plasmas* **1**, 2682 (1994).
- [33] H. Sugama and W. Horton, *Phys. Plasmas* **5**, 2560 (1998).
- [34] A. G. Peeters, C. Angioni, and D. Strintzi, *Phys. Rev. Lett.* **98**, 265003 (2007).
- [35] G. Tardini *et al.*, *Nucl. Fusion* **49**, 085010 (2009).
- [36] To give an idea of the complexity of the theoretical problem, we point out that the poloidal velocity will not be counterclockwise at low collisionality, as suggested by Fig. 1, but clockwise due to the collisional friction between particles of the type sketched in Fig. 1 and a population of trapped particles [26]. Determining the toroidal rotation requires even more work than the poloidal velocity, and the finite-orbit-width effects come in through other mechanisms. For example, the poloidal velocity breaks the up-down symmetry and gives a preferred direction to the turbulent and collisional transport of toroidal angular momentum.
- [37] P. J. Catto and A. N. Simakov, *Phys. Plasmas* **12**, 012501 (2005).
- [38] S. K. Wong and V. S. Chan, *Phys. Plasmas* **16**, 122507 (2009).
- [39] M. F. F. Nave *et al.*, *Plasma Phys. Controlled Fusion* (to be published).
- [40] The data for TCV was obtained from [7]. In that article, the authors plotted the velocity at the magnetic axis multiplied by  $I_p$  against the temperature at the magnetic axis. This is approximately the same as  $I_p \Delta V_\phi$  vs  $\Delta T_i$  because both the rotation and the temperature at the edge are small compared to their values at the magnetic axis.
- [41] F. W. Perkins *et al.*, *Phys. Plasmas* **8**, 2181 (2001).
- [42] L.-G. Eriksson and F. Porcelli, *Nucl. Fusion* **42**, 959 (2002).
- [43] J. S. deGrassie *et al.*, *Nucl. Fusion* **49**, 085020 (2009).
- [44] F. J. Casson *et al.*, *Phys. Plasmas* **16**, 092303 (2009).
- [45] M. Barnes *et al.*, *Phys. Rev. Lett.* **106**, 175004 (2011).
- [46] E. G. Highcock *et al.*, *Phys. Rev. Lett.* **105**, 215003 (2010).
- [47] E. G. Highcock *et al.*, *Phys. Plasmas* **18**, 102304 (2011).
- [48] See F. Romanelli and R. Kamendje, *Nucl. Fusion* **49**, 104006 (2009). (All members of the JET-EFDA Collaboration appear in the appendix of this paper.)